

CubeP Crowds: crowd simulation integrated into “Physiology-Psychology-Physics” factors

Mingliang Xu, Chaochao Li, Pei Lv, Wei Chen, Zhigang Deng, Bing Zhou and Dinesh Manocha

Abstract—In this paper, we present a novel CubeP model for crowd simulation that comprehensively considers physiological, psychological, and physical factors. Inspired by the theory of “the devoted actor”, our model determines the movement of each individual by modeling the physical influence from physical strength and emotion. In particular, human physical strength is efficiently computed with a physiology-based method. Inspired by James-Lange theory, the emotion is determined by means of an enhanced susceptible-infectious-recovered model that leverages the inherent relation between the physical strength and the psychological emotion. As far as we know, this is the first time that we integrate physiological, psychological, and physical factors together in a unified manner, and the relationship between each other is explicitly determined. The results and comparisons with real-world video sequences verify that the new model is capable of generating effects similar to real-world scenarios. It can also reliably predict the changes in the physical strength and emotion of individuals in an emergency situation. We evaluate and validate the performance of our model in different scenarios.

Index Terms—Crowd simulation, emotional contagion, physical strength, James-Lange theory



1 INTRODUCTION

WITH rapid economic and social development, the number of large-scale crowd activities and events has increased considerably. Mass disturbances can cause serious economic and social harm due to their uncertainty and high risk [1]. Therefore, in recent years, researchers have focused on emotional evolution, energy consumption, and behavior decisions among crowds in an emergency situation. Safe and efficient crowd simulation has become one of the most important research topics in the field of computer graphics and public safety [2].

The main purpose of crowd simulation algorithms is to model the movement of individuals in a crowd realistically under emergency situations [3]. The individual movement in terms of speed and direction represents the physical state of those individuals in a crowd [4]. To model individual movement realistically, some crowd simulation algorithms involve a human physiological factor: physical strength [5]. Physical strength directly affects the moving speed of an individual [6]. Moreover, some approaches try to consider the emotion of individual in crowd simulation, which is one of the most commonly used psychological factors [7]. Researchers find that the occurrence of danger can directly cause emotional changes in an individual, thereby further affecting its movement [8], [9]. However, describing the inherent relationship between physical strength and emotion

is difficult as well as combining these factors to determine the movement of each individual [10]. These three factors (individual movement, physical strength, and emotion) in crowd movement influence one another and evolve dynamically. Therefore, modeling them in a unified model for crowd simulation is challenging, as described in the following:

(1) Accurately modeling the physical strength of an individual in a crowd is difficult. This task involves considering many factors that are needed to quantify the influence of physical strength on crowd movement [5].

(2) Modeling the individual emotion in a crowd accurately is difficult because of its constantly dynamical changes [11]. Various factors, such as personality, physical strength, and individual movement, affect emotions.

(3) The quantitative relationship among the physical, physiological, and psychological factors in crowd movement has not been exploited in a unified manner. Most previous methods only consider the physiological or psychological factor, but have not tried to combine it with other issues that govern the behavior or movement [12], [13].

To address these challenges, a novel, comprehensive crowd simulation model that integrates factors of psychology, physiology, and physics is proposed in this paper. Firstly, we present an efficient method for physical strength calculation based on the idea of how individuals work in physics in a crowd. Secondly, inspired by James-Lange theory [10], we improve the traditional emotional contagion mechanism mentioned in [7], [14] for emotion calculation, which describes the influence of physical strength on emotion. Finally, inspired by the theory of “the devoted actor” [15], which shows that both psychological state and physiological state have effects on an individual’s physical state, we present a comprehensive model that combines the physiological, psychological, and physical factors in a unified manner (shown in Figure 1). The strenuous movement of individuals is often observed in emergency or evacuation

- *Mingliang Xu, Chaochao Li, Pei Lv, and Bing Zhou are with Center for Interdisciplinary Information Science Research, ZhengZhou University, 450000.*
- *Wei Chen is with State Key Lab of CAD&CG, Zhejiang University, 310058.*
- *Zhigang Deng is with Department of Computer Science, University of Houston, Houston, TX, 77204-3010.*
- *Dinesh Manocha is with Department of Computer Science, University of North Carolina, Chapel Hill, NC, USA.*
E-mail: {*iexumingliang, ielvpei, iebzhou*}@zzu.edu.cn;
zgulcc@gs.zzu.edu.cn; chenwei@cad.zju.edu.cn; zdeng4@uh.edu; dm@cs.unc.edu

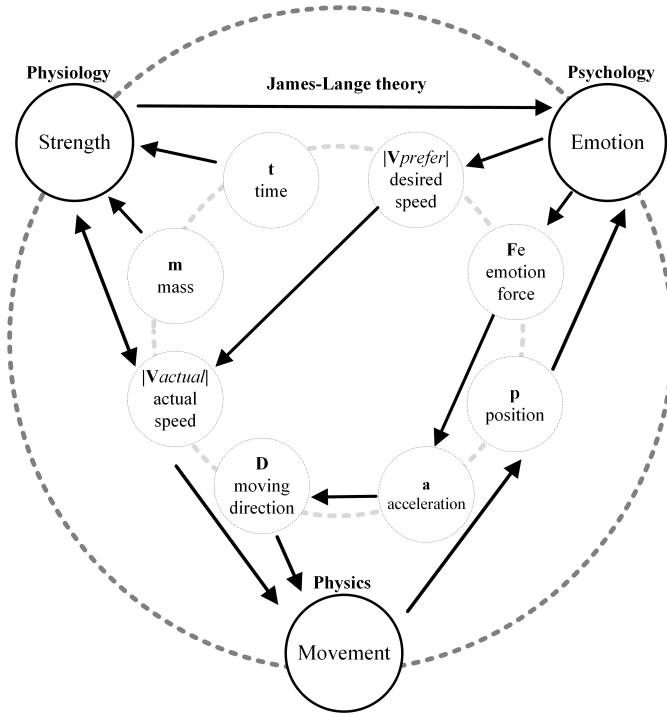


Fig. 1: The relationships among the physiological (strength), psychological (emotion), and physical (movement) factors of moving individuals in a crowd. The physical strength consumption is calculated according to the actual speed, mass, and moving time of individuals. The panic emotion is determined by the position and physical strength of the individual, and it will further affect the individual’s desired speed. Moreover, the human’s current emotion will affect each individual’s moving direction by changing its acceleration based on the inferred emotion force. These three factors are affected by one another and we highlight their combined effect on the crowd’s movement.

situations, and the relationship between these factors is more obvious in such situations than that of other ones. Thus, in this paper, we mainly focus on simulating crowd movement in such emergency situations.

The contributions of this paper are summarized as follows:

- We introduce a new physical strength calculation method based on the idea of how individuals do work in physics and also characterize its dynamical changes quantitatively [5], [16].
- We improve the traditional epidemiological SIR model based on James-Lange theory [10]. The new proposed emotion model not only analyzes emotional contagion and attenuation, but also depicts the relationship between physical strength and emotion.
- As far as we know, this is the first time that we propose a comprehensive crowd simulation model that considers the physical strength and emotion factors in emergency or evacuation situations using the aforementioned two models.

The rest of this paper is organized as follows. Background and related work are reviewed in Section 2. The

definition of our proposed crowd simulation model is introduced in Section 3. Experiments are presented in Section 4. Finally, this paper is concluded in Section 5.

2 RELATED WORK

In this section, we provide a brief overview of prior work on crowd simulation based on whether such work involves physical, psychological, and physiological factors.

2.1 Traditional crowd simulation models

We summarize important crowd simulation models without considering psychological or physiological factors [17], [18], [19], [20], [21] in this subsection.

In the real world, many environmental factors influence the individual movement, i.e., scene layout, moving pedestrians, and stationary groups [22], [23], [24]. During the evacuation of the crowd, the behavioral choice of an individual is highly dependent on the moving directions of nearby individuals, the hazard location, and obstacles [25]. To realize better behavioral choices, most approaches calculate the position of each individual at the next time step to obtain a conflict-free moving path in global scenario [26]. However, these approaches are not applicable to the highly complex and huge scene with dense crowd since it has many restrictive conditions of different obstacle. Other approaches use local obstacle avoidance methods. Namely, once the movement state of an individual is determined, the movement states of other individuals are updated by iterating the premise of collision avoidance [27].

Unfortunately, the aforementioned approaches still face difficulty in accurately controlling the individual movement. Researchers in this field are increasingly focusing on integrating global path planning and local obstacle avoidance together [28], [29], [30]. Tomer Weiss et al. [31] model collision avoidance constraints both in short-range and long-range to deal with sparse and dense crowds. In [32], intergroup- and intragroup-level techniques are presented to perform coherent and collision-free navigation using reciprocal collision avoidance. Mutual information of the dynamic crowd is used to guide agents’ movement combining both macroscopic and microscopic controls [33]. By constructing a visual tree, the shortest path without collision is obtained in [34]. In addition, in [35], [36], [37], and [38], path planning and navigating algorithm in complex contexts are described for crowd simulation. Furthermore, in [39], an effective long-range collision avoidance algorithm is proposed.

Different from the aforementioned work, the present study enhances the traditional social force model to avoid collisions with surrounding individuals and obstacles by involving emotional and physical strength calculations together. This approach is not concerned with traditional crowd simulation models.

2.2 Crowd simulation with emotion (psychologically)

The psychological state of an individual plays a vital role in his or her decision-making process [40], [41]. Emotion is a typical and unstable psychological parameter, which has a great influence on individuals in a crowd. In this subsection,

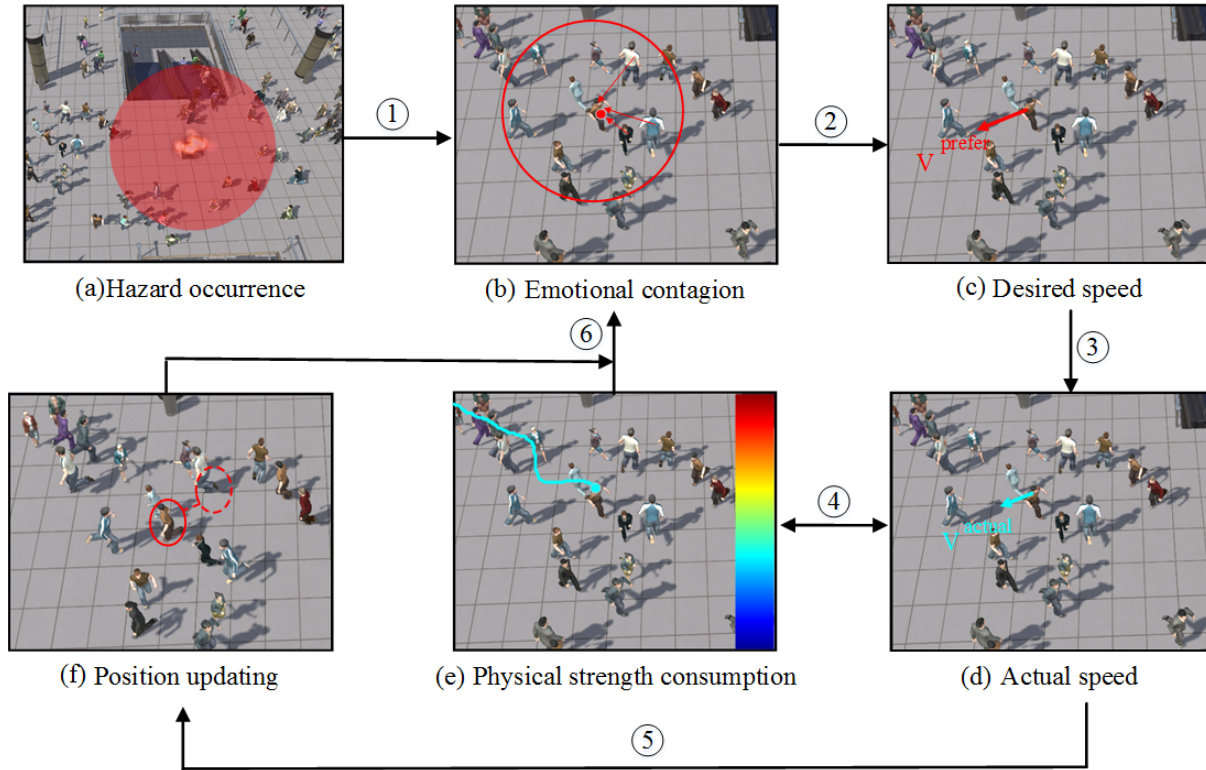


Fig. 2: The flowchart of the CubeP model. (a) A hazard occurs and the red area represents the range of influence of the hazard. (b) The emotional changes of one individual are calculated according to the direct impact of the hazard and emotional contagion of his neighbors (Section 3.3). (c) The desired speed and direction of each individual [8] are calculated based on updated emotion (Section 3.4). (d) Due to the limit of physical strength consumption, the actual speed is further determined [6] (Section 3.4). (e) Different color represents different physical strength consumption. The actual speed affects the physical strength consumption (Section 3.2). On the contrary, the cumulative physical strength consumption also determines the actual maximal speed of the individual at the next time step (Section 3.4). The current physical strength consumption reflects the emotional experience of an individual [10] (Section 3.3). (f) The position of the individual is updated according to its actual speed, and the new position causes emotional changes again (Section 3.3).

we mainly introduce representative work about emotion and its role in crowd simulation.

The epidemiological SIR model [42] divides the individuals in a crowd into three categories: infected, susceptible, and recovered. The spread of disease among these three groups is analyzed. This model has also been extended to other different fields. In [43], the extended model is used to simulate the spread of rumor. Some researchers use the epidemiological SIR model in conjunction with other models to describe emotion propagation under specific situations. In [44], dynamic emotion propagation is described from the perspective of social psychology with a combination of thermodynamic-based models and epidemiological-based models. The cellular automata model is used to simulate the spread of infectious diseases in [45]. In [7], the epidemiological SIR model is improved by combination with the OCEAN model.

The phenomenon of emotional contagion occurs more obviously in a panic crowd. In [46], a qualitatively simulated approach to model emotional contagion is proposed for a large-scale emergency evacuation. This approach confirms that the effectiveness of rescue guidance is influenced by the leading emotion in the crowds. Moreover, the cellular automata model based on the SIR model (CA-SIRS) is used

in [47] to describe emotional contagion in the crowd-moving process under an emergency situation.

Inspired by the James-Lange theory in biological psychology, we improve the traditional epidemiological SIR model by considering the influence of physical strength on emotion. In contrast to previous methods considering emotion only, we further demonstrate the relationship between physical strength and emotion.

2.3 Crowd simulation with physical strength (physiologically)

To complete a comprehensive analysis of crowd movement, not only psychological factors, but also physiological factors of individuals should be considered because physiological factors are also very important in determining the crowd movement [6]. Physical strength is one of the most important physiological parameters that affect individual movement. Bruneau et al. [48] apply the principle of minimum energy (PME) on groups of different sizes and densities. In [49], [50], some physiological indicators (such as physical strength consumption and heart rate) are described. Furthermore, the relationship between physical strength consumption and heart rate is revealed, which is also a method

for predicting physical strength consumption based on the heart rate during moderate exercise and vigorous exercise. In [5], a calculation method of the physical strength consumption for disabled individuals is introduced. The work in [6] shows that the relationship between physical strength and speed is nonlinear. This finding shows that small changes in physical strength can exert substantial movement effects on frail adults, whereas significant changes in physical strength have a minimal effect on healthy adults. In [5], the researchers investigate how the cumulative consumption of physical strength affects the evacuating time of individuals. Guy et al. [16] propose the principle of least effort (PLE) to compute physical strength consumption of some movement in the form of doing work in physics by individuals. Furthermore, Guy et al. [51] propose a less energy-consuming, conflict-free crowd movement method based on the criterion of minimal physical strength consumption [16].

The aforementioned approaches discuss the relationship between physical strength and other physiological parameters (heart rate and oxygen uptake, for example). In this paper, based on prior approaches, we also describe the effect of physical strength on the physical movement of individuals. Moreover, we analyze the relationship between physical strength and emotion by emphasizing the interaction of individual physiological, psychological, and physical states.

3 CUBE-P-CROWDS MODEL

The crowd simulation model proposed in this paper that comprehensively considers the physiological, psychological, and physical factors, is named by CubeP-Crowds Model (CubeP for short). The flow chart of the CubeP model is presented in Figure 2.

The CubeP model consists of three important components: physical strength, panic emotion, and individual movement. The human physical strength is efficiently computed with a physiology-based method (Section 3.2). The panic emotion is determined by means of an enhanced susceptible-infectious-recovered (SIR) model that leverages the inherent relation between the physical strength and the psychological emotion (Section 3.3). The CubeP model computes the movement of an individual by modeling the physical influence from the physical strength and the emotion (Section 3.4).

3.1 Symbols and Notation

For convenience, the important parameters and their descriptions used in the CubeP model are listed in Table 1.

3.2 Physical strength calculation

Physical strength is one of the most commonly used physiological indicators and is closely related to the individual movement. It is defined in the following equation:

$$P(t) = P_{hor}(t) + P_{ver}(t) \quad (1)$$

where $P(t)$ denotes the total physical strength consumption at time t , and $P_{hor}(t)$, $P_{ver}(t)$ denote the physical strength consumption along the horizontal and vertical directions separately. They are defined as follows:

TABLE 1: The parameters used in the CubeP model.

Notation	Description
$P(t)$	Physical strength consumption at time t
$P_{hor}(t)$	Physical strength consumption along the horizontal direction at time t
$P_{ver}(t)$	Physical strength consumption along the vertical direction at time t
F^x	Driving force of individual along the horizontal direction
F^y	Pulling force of individual along the vertical direction
E	Panic emotion
E_o	Emotional cognitive component
E_p	Emotional experience component
T_1	If the emotion of an individual exceeds this threshold T_1 , the individual will be infected.
T_2	If the emotion of an individual surpasses this threshold T_2 , the individual is capable of spreading the emotion to his neighboring individuals.
E_o^h	The emotion is effected from hazard.
E_o^c	Emotional contagion
E_o^d	Emotional attenuation
EE	Energy expenditure
$V_i(t)$	Moving direction of the individual i at time t
$V_i^s(P, t)$	Safety evacuation direction of the individual i at position P and at time t
$V_i^{round}(t)$	Combined moving directions of individuals who are in the perceived range of the individual i at time t
v_i^{prefer}	The desired speed v_i^{prefer} of the individual i considers only the emotion factor.
v_i^{actual}	The actual speed v_i^{actual} of the individual i is limited by his own physical strength.
v^p	Maximum speed v^p according to current physical strength consumption
v_i^{MAX}	Maximum speed that the individual i can run
v_i^{NOR}	Speed of the individual i in the normal case (emotion value is equal to zero)

$$P_{hor}(t) = \sum_{i=1}^t F^x \cdot d \quad (2)$$

$$P_{ver}(t) = \sum_{i=1}^t F^y \cdot h \quad (3)$$

F^x is the driving force of the individual along the horizontal direction. This force overcomes friction. d is the moving distance of the individual at time t . $F^x \cdot d$ represents the work done by the individual along the horizontal direction. F^y is the pulling force of the individual along the vertical direction. This force overcomes gravity. h is the rising height of the individual at time t , and $F^y \cdot h$ represents the work done by the individual along the vertical direction.

According to the laws of physics, F^x is defined as follows:

$$F^x = f + \frac{(v_i^x - v_{i-1}^x)m}{\tau} \quad (4)$$

A diagram of the physical strength calculation is shown in Figure 3.

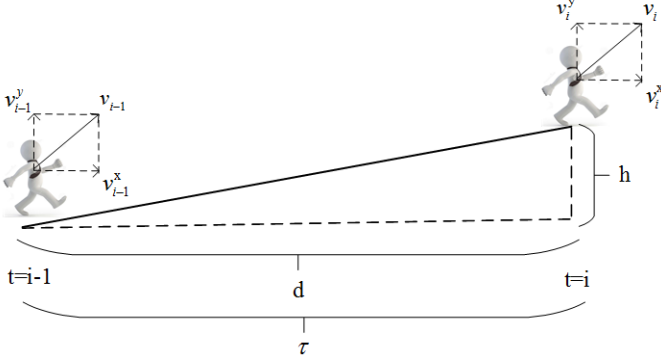


Fig. 3: Schematic of physical strength calculation. v_i^x is the velocity component of an individual in the horizontal direction at time i , and the length of each time step is τ . The horizontal speed of the individual changes from v_{i-1}^x to v_i^x in time interval τ . f is the friction in the horizontal direction.

The friction f is defined in Equation 5, k is defined in Equation 6, and t is defined in Equation 7 according to [52], [53]. μ is the friction factor, which is related to the shoes and the ground. In our implementation, $\mu=0.58$ is adopted, which is also recommended in [54]. v is the current velocity magnitude, v_{min} is the minimal velocity magnitude, and v_{max} is the maximal velocity magnitude.

$$f = t \cdot \mu \cdot mg \cdot k \quad (5)$$

$$k = 1.5 + 0.5 \cdot \frac{v - v_{min}}{v_{max} - v_{min}} \quad (6)$$

$$t = 0.6 - 0.2 \cdot \frac{v - v_{min}}{v_{max} - v_{min}} \quad (7)$$

The physical strength consumption in the horizontal direction is defined by:

$$P_{hor}(t) = \frac{1}{2} \cdot \sum_{i=1}^t \left\{ \left((v_i^x)^2 - (v_{i-1}^x)^2 \right) m + t \cdot \mu \cdot mg \cdot k (v_i^x + v_{i-1}^x) \tau \right\} \quad (8)$$

According to the laws of physics, F^y is defined by the following equation:

$$F^y = mg + \frac{(v_i^y - v_{i-1}^y)m}{\tau} \quad (9)$$

where v_i^y is the velocity component in the vertical direction at time i .

The physical strength consumption in the vertical direction is defined by:

$$P_{ver}(t) = \frac{1}{2} \cdot \sum_{i=1}^t \left\{ \left((v_i^y)^2 - (v_{i-1}^y)^2 \right) m + (v_i^y + v_{i-1}^y) mg \tau \right\} \quad (10)$$

3.3 Emotion calculation affected by physical strength

This section presents the emotion calculation method of an individual. The emotion E consists of two components. The first one is emotional cognitive component E_o , which relates to the hazard, emotional contagion, and emotional attenuation. The second is emotional experience component E_p , which is calculated using physical strength and heart rate. Therefore, the final emotion value is defined as follows:

$$E = w \cdot E_o + (1 - w) \cdot E_p \quad (11)$$

where w is weighting parameter, and $0 < w < 1$.

3.3.1 The emotional cognitive component

During the evacuation, individuals can be in one of two states: susceptible or infected. When the emotion of an individual exceeds a certain threshold T_1 , the individual will be infected. If the emotion intensity of an individual surpasses another threshold T_2 , then the individual is capable of spreading the emotion to its neighboring individuals. In general case, $T_1 < T_2$. T_1 and T_2 are correlated with individual personality. Here, we represent the personality of individuals using the "OCEAN" personality model [7]. The personality is represented by a five-dimensional vector $\langle O, C, E, A, N \rangle$. T_1 and T_2 are defined by the following:

$$T_1 = \alpha \cdot C - \beta \cdot N + \gamma \quad (12)$$

where $T_1 \propto^{-1} N$, $T_1 \propto C$, and $T_1 \in [0,1]$.

$$T_2 = \delta - \xi \cdot E \quad (13)$$

where $T_2 \propto^{-1} E$ and $T_2 \in [0,1]$.

E_o consists of three terms: effect from hazard E_o^h , emotional contagion E_o^c , and emotional attenuation E_o^d .

When individuals are able to perceive a hazard, they may be infected. E_o^h is defined as follows:

$$\Gamma_s(P, t) = \begin{cases} \frac{\alpha}{\sqrt{2\pi} \cdot r_s} e^{-\frac{(P-P_s)^2}{2r_s^2}} & \text{if } \|P - P_s\| < r_s \text{ and } t \in U \\ 0 & \text{otherwise} \end{cases} \quad (14)$$

$$E_o^h(P, t) = \sum_{s=0}^{n-1} \Gamma_s(P, t) \quad (15)$$

where P is the position of individual, P_s is the position of hazard, r_s is the radius of influence range of hazard, U is the duration of hazard, and $\alpha(\alpha > 0)$ represents the strength of hazard.

In a crowded place, an individual can perceive the behavior of others within a certain distance. Within the perceptual range, when a susceptible individual i sees an expressive individual j (the emotion value is higher than threshold T_2), i gets exposed by receiving a random dose d_i from a specified probability distribution multiplied by the emotion intensity of j . We denote the emotion value of individual j at the time t' as $e_j(t')$. The emotion value perceived by individual i due to emotional contagion is defined in Equation 16.

$$E_{i,o}^c(P, t) = \sum_{t'=0}^t \sum_{\forall j | j \in \text{Visibility}(i) \wedge j \text{ is expressive}} d_i(t') e_j(t') \quad (16)$$

Emotional attenuation is defined in Equation 17.

$$E_o^d(P, t) = E_o(P^{pre}, t-1) \cdot \eta \quad (17)$$

where $E_o^d(P, t)$ is the decay function of the emotion and η is the decay rate. η is positively related to the individual personality factor N , and it is defined as follows:

$$\eta(t) = \begin{cases} 0 & t < t_1 \\ \frac{e^{\beta_2(t-t_2)} - e^{\beta_2(t-1-t_2)}}{1 + e^{\beta_2(t-t_2)}} + \alpha \cdot N & t \geq t_1 \end{cases} \quad (18)$$

where $\beta_2 > 0$ and $\eta \propto N$.

The change of emotional cognitive component $\Delta E_o(P, t)$ is defined in Equation 19. The E_o is defined in Equation 20.

$$\Delta E_o(P, t) = E_o^h(P, t) + E_o^c(P, t) - E_o^d(P, t) \quad (19)$$

$$E_o(P, t) = E_o(P^{pre}, t-1) + \Delta E_o(P, t) \quad (20)$$

3.3.2 The emotional experience component

In this section, we present the calculation method of E_p . Individual emotion undergoes three stages: cognition, action, and experience. An event occurs first, and the individual perceives the current scene (emotional cognitive stage). Subsequently, the individual takes the corresponding actions with physiological changes (action stage). Finally, the individual has the emotional experience (experience stage).

Under emergency situations, once a hazard occurs, the individuals around it take different actions immediately. This will bring the physical strength consumption. The energy expenditure (physical strength consumption in a minute) is chosen as the measure of physiological changes. The current heart rate is calculated using the energy expenditure. Then, the increment of the emotional experience value is calculated based on the increment of heart rate. Thereafter, the current emotional experience value E_p is obtained. The details of the calculation method are as follows.

The energy expenditure EE can be computed by Equation 21 under the situation where individuals experience panic to escape from the hazard [50].

$$EE = gender \times (-55.0969 + 0.6309 \times HR + 0.1988 \times weight + 0.2017 \times age) + (1 - gender) \times (-20.4022 + 0.4472 \times HR - 0.1263 \times weight + 0.074 \times age) \quad (21)$$

where $gender=1$ for males and 0 for females, age (year) $\in [19,45]$, and $weight$ (kg) $\in [47,116]$. Equation 21 describes the relationship between energy expenditure (KJ/min) and heart rate (beat/min).

Furthermore, according to [55], the heart rate (HR) and intensity of anxiety or fear (emotional experience) are positively correlated. In [55], before and after an electric shock, the heart rate is recorded by minute, and panic emotional experience is reported once per minute. ΔE_p and ΔHR are the increments of emotional experience and heart rate compared with the values before the test.

Using the curve fitting method, we can obtain the relationship between ΔHR and ΔE_p .

$$\Delta E_p = 0.03669 \cdot \Delta HR - 0.0724 \quad (22)$$

E_p is defined in Equation 23 and $E_p(0) = 0$.

$$E_p(t) = E_p(t-1) + \Delta E_p(t) \quad (23)$$

3.4 Individual movement model

Based on the results of physical strength and emotion, the movement of each individual can be determined accurately in two aspects of moving direction and moving speed.

3.4.1 Moving direction

When hazard occurs, individuals who are able to perceive the hazard directly will fall into an infected state and will calculate their own safety evacuation direction $V_i^s(P, t)$. $V_i^{round}(t)$ is the combined moving directions of individuals who are in the perceived range of the individual i . At the same time, individuals whose emotion exceeds the threshold T_2 will have the ability to express this panic emotion.

$$V_i^s(P, t) = \begin{cases} \sum_{s=0}^{n-1} \Gamma_s(P, t) \cdot \vec{P}_s & \text{if } \|P - P_s\| < r_s \text{ and } t \in U \\ \vec{V} & \text{otherwise} \end{cases} \quad (24)$$

$$V_i^{round}(t) = \sum_{\forall j | j \in \text{Visibility}(i) \wedge j \text{ is expressive}} V_j(t) \quad (25)$$

Finally, the moving direction $V_i(t)$ of an individual who directly perceives the hazard is defined as follows:

$$V_i(t) = E \cdot V_i^s(P, t) + (1 - E) \cdot V_i^{round}(t) \quad (26)$$

where E is the emotion value. The moving direction of individual i is influenced by panic emotion, safety evacuation direction, and other neighboring panicked individuals.

Individual i is able to perceive the hazard indirectly by being infected by surrounding individuals when his emotion E exceeds the threshold T_1 . The infected individual i moves in the direction of $V_i(t)$, as shown in Equation 27. $V_i^{old}(t)$ is the moving direction of the individual i at the last moment when he is not in panic. The more panicked the individual is, the more easily he moves with other neighboring panicked individuals. Nonetheless, uninfected individuals still move in their original directions.

$$V_i(t) = (1 - E) \cdot V_i^{old}(t) + E \cdot V_i^{round}(t) \quad (27)$$

3.4.2 Moving speed

In panic situation, the speed of an individual i is expressed by the following equation [8]:

$$v_i^{prefer} = (1 - E) \cdot v_i^{NOR} + E \cdot v_i^{MAX} \quad (28)$$

where v_i^{prefer} is the speed considering only the emotion factor, and $0 \leq E \leq 1$. The speed of the individuals in the normal case (the emotion value is equal to zero) is v_i^{NOR} , and the maximal speed is v_i^{MAX} . The more panicked an individual is, the larger his speed is.

However, an individual is limited by his own physical strength. In some cases, the moving speed of an individual cannot reach the desired speed due to the maximum limited by current physical strength consumption. The actual speed cannot exceed the maximal speed v^p .

$$v_i^{actual} = \min(v_i^{prefer}, v^p) \quad (29)$$

The dependence of the decay rate and maximal speed on physical strength is presented in Table 2.

The actual speed can be calculated in Equation 30.

$$v_i^{actual} = \min((1 - E) \cdot v_i^{NOR} + E \cdot v_i^{MAX}, v_i^{MAX} \cdot \xi) \quad (30)$$

TABLE 2: Dependence of speed decay rate and maximal-limit speed on physical strength. Along with the consumption of physical strength, the maximal-limit speed decreases.

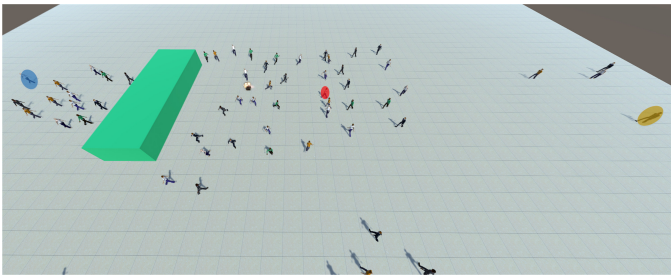
Physical strength consumption p (J)	Decay rate ξ (%)	Maximal-limit speed v^p (m/s)
0 – 20154	100.00	v_i^{MAX}
20154 – 40279.6713	99.85	$v_i^{MAX} \cdot 0.9985$
40279.6713 – 81121.0042	89.42	$v_i^{MAX} \cdot 0.8942$
81121.0042 – 166258.892	75.8	$v_i^{MAX} \cdot 0.758$
166258.892 – 181569.609	69.82	$v_i^{MAX} \cdot 0.6982$
181569.609 – 196355.176	65.72	$v_i^{MAX} \cdot 0.6572$

4 EXPERIMENTS

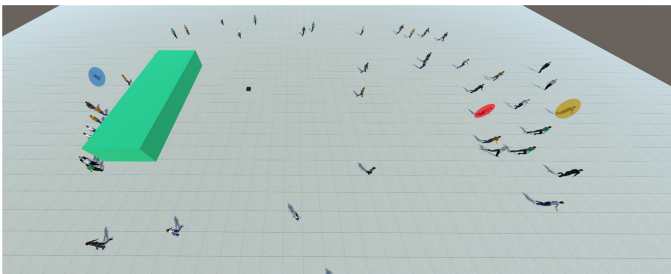
Our proposed algorithm is used to simulate crowd movement in various scenarios. We demonstrate the benefits of our model in different scenarios. The simulation results show that our proposed method can generate realistic group behavior. It can also reliably predict the changes of physical strength and emotion of a crowd in an emergency.

4.1 Relationship evaluation among emotion, physical strength, and moving speed

To validate our model, we analyze the emotion and speed of different individuals with and without considering the physical strength factor in a virtual crowd scene (shown in Figure 4). Then, the impact of different initial values of physical strength on the emotion and speed is analyzed.



(a) Positions of the individuals at the 10th frame when the hazard occurs



(b) Positions of the individuals at the 80th frame after the hazard occurred

Fig. 4: A virtual simulation scene. The green cube represents the obstacle. The red ellipse is individual No. 10, the yellow one is No. 35, and the blue one is No. 56. Individual No. 10 can be aware of the hazard directly, individual No. 35 is able to perceive the hazard through the emotional contagion indirectly, and individual No. 56 will not be affected by the hazard directly or indirectly.

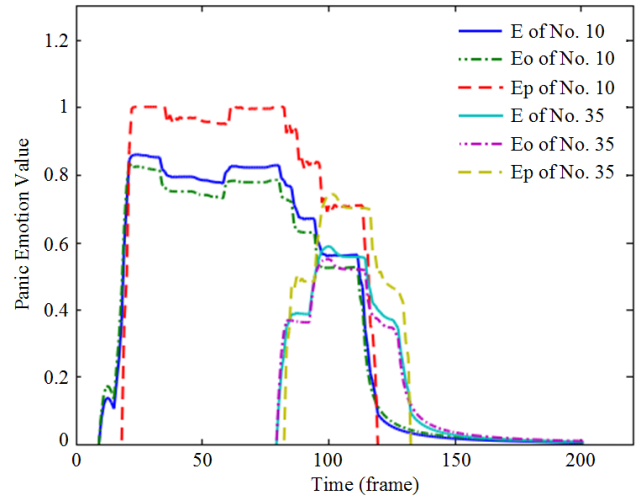


Fig. 5: Emotion values of individuals No. 10 and No. 35. E_p is larger than E_o . The emotion value of individual No. 10 is larger than that of individual No. 35. The duration of panic emotion of individual No. 10 is also longer than that of individual No. 35.

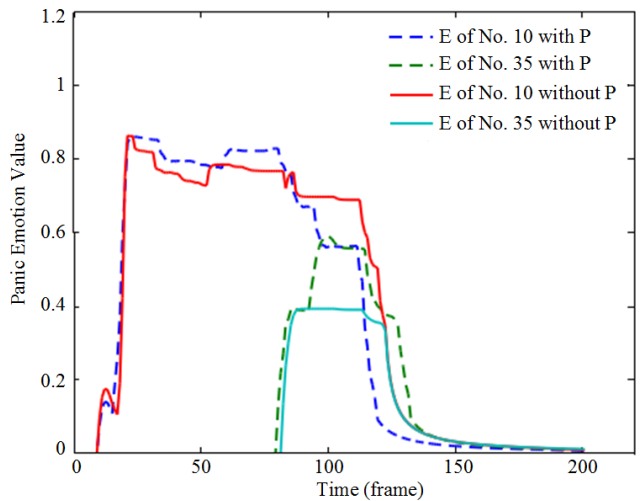


Fig. 6: Emotions of individuals No. 10 and No. 35 with and without considering the physical strength factor. The emotion value of individuals whose physical strength factor is considered is higher than that of individuals whose physical strength factor is not considered.

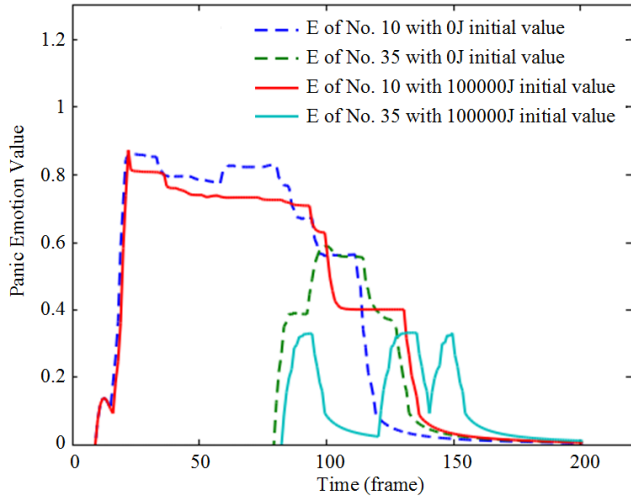


Fig. 7: Emotions of individuals with different initial values of physical strength. The emotion of the individual with 100000J initial value of physical strength consumption is less than the emotion of individual with 0J initial value of physical strength consumption.

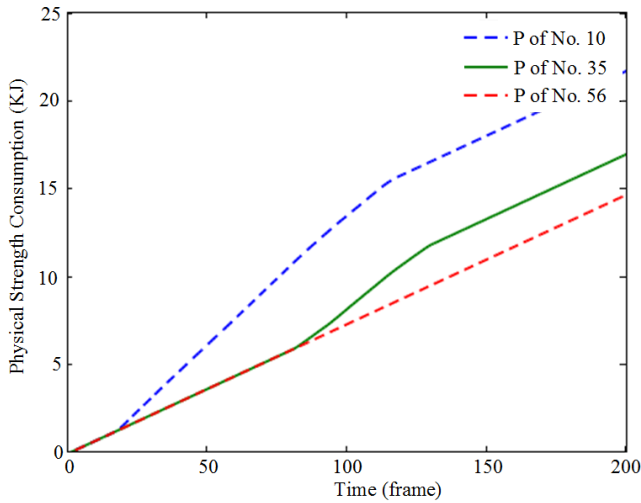


Fig. 8: Physical strength consumption of individuals. Individual No. 10 is more frightened than the other two and his moving speed is faster, so he consumes more physical strength than the other two. Moreover, the slope of his physical strength consumption is also larger than that of the other individuals. Since individual No. 56 is not panicked, the slope of his physical strength consumption does not change.

Three individuals in this scene, namely, No. 10, No. 35, and No. 56 are taken as examples. The emotional changes of individual No. 10 and No. 35 in the above scene are presented in Figure 5. Compared with individual No. 35, individual No. 10 can perceive the hazard directly and is closer to the hazard, so he is more panicked than individual No. 35.

The emotion of different individuals with and without considering the physical strength factor are shown in Figure

6. As mentioned, physical strength consumption affects emotional experience. Therefore, without considering the physical strength, the emotional experience becomes zero and the final emotion does not accumulate this component. Thus, emotion value considering physical strength factor is higher.

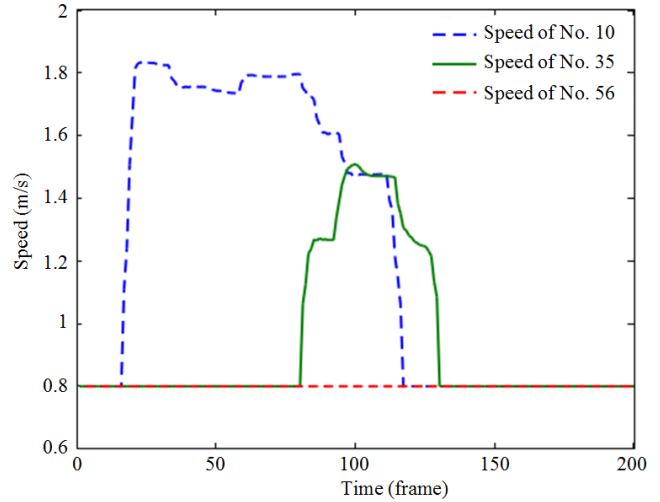


Fig. 9: The moving speed of different individuals. Individual No. 56 is not panicked. Thus, his moving speed does not change. The remaining two individuals start to move faster when they become panicked. Since individual No. 10 is more panicked than individual No. 35, he moves faster.

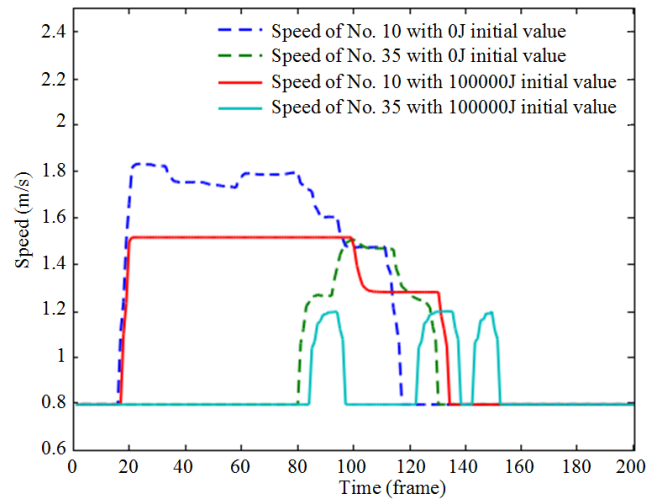


Fig. 10: The speed of individuals with different initial values of physical strength consumption. The individual with 0J initial value of physical strength consumption moves faster than the individual with 100000J initial value of physical strength consumption.

The emotion of individuals with different initial values of physical strength consumption are presented in Figure 7. If an individual has consumed too much physical strength (initial value of physical strength consumption is 100000J), the rest of his physical strength will be reduced. Thus, the

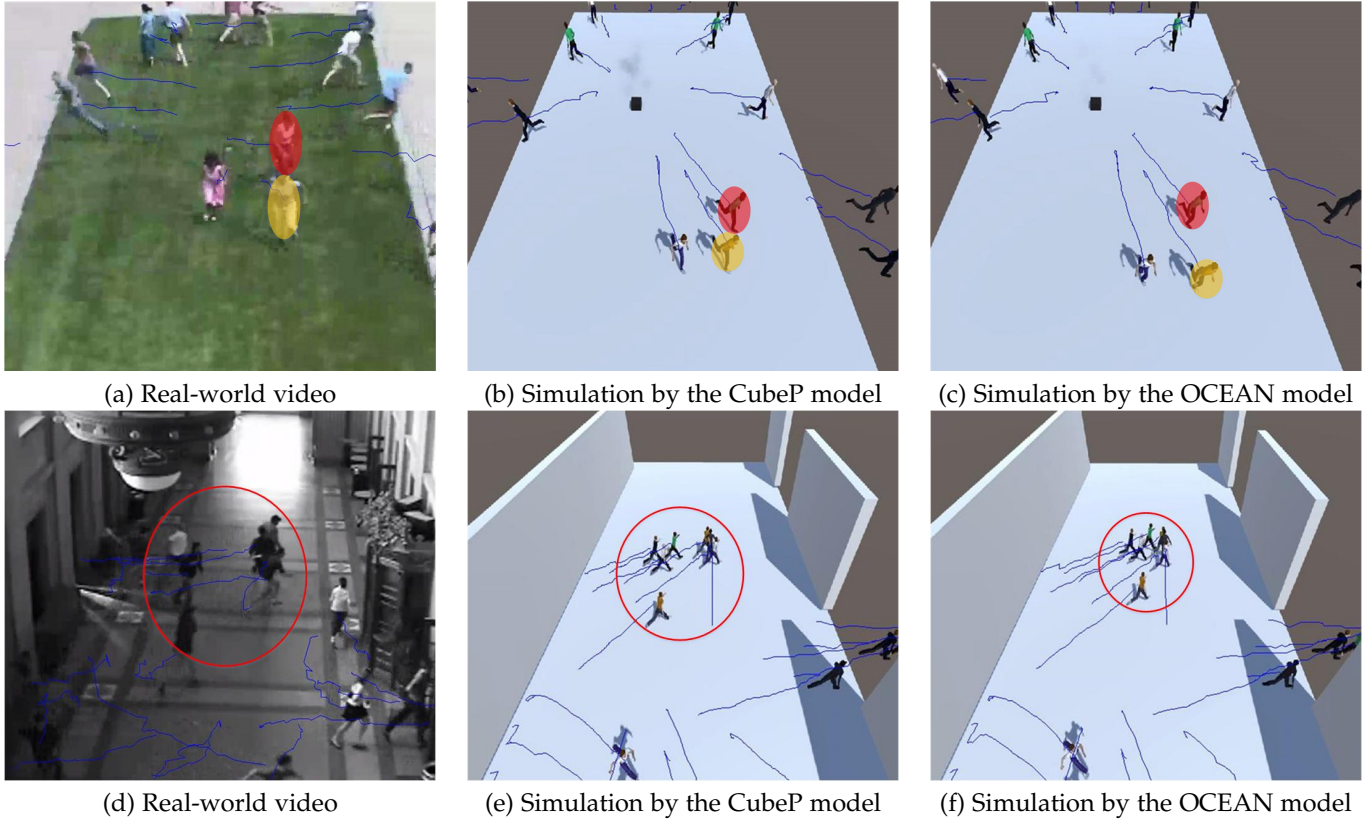


Fig. 11: Comparison between real scenes and simulation results by different models. (a) and (d) are real scenes, and (b), (c), (e), (f) are simulation results. Each row represents one scene. (a) The red ellipse is individual No. 1 and the yellow one is individual No. 2. The individual No. 1 gets closer to the individual No. 2. We present the line charts to show the distance between individual No. 1 and individual No. 2 at different time steps (Figure 12a). (b) As the speed is influenced by physical strength, simulating the situation where individual No. 1 gets closer to individual No. 2 is easier by the CubeP model. (f) The simulation trajectories of different individuals in the red circle by the OCEAN model are similar and individuals easily get together, which is different from the real-world video. We provide the line charts to show the collectiveness [56], [57] of simulation results and real-world video at different time steps (Figure 12b). The collectiveness of simulation by the OCEAN model is much higher than that of the real-world video.

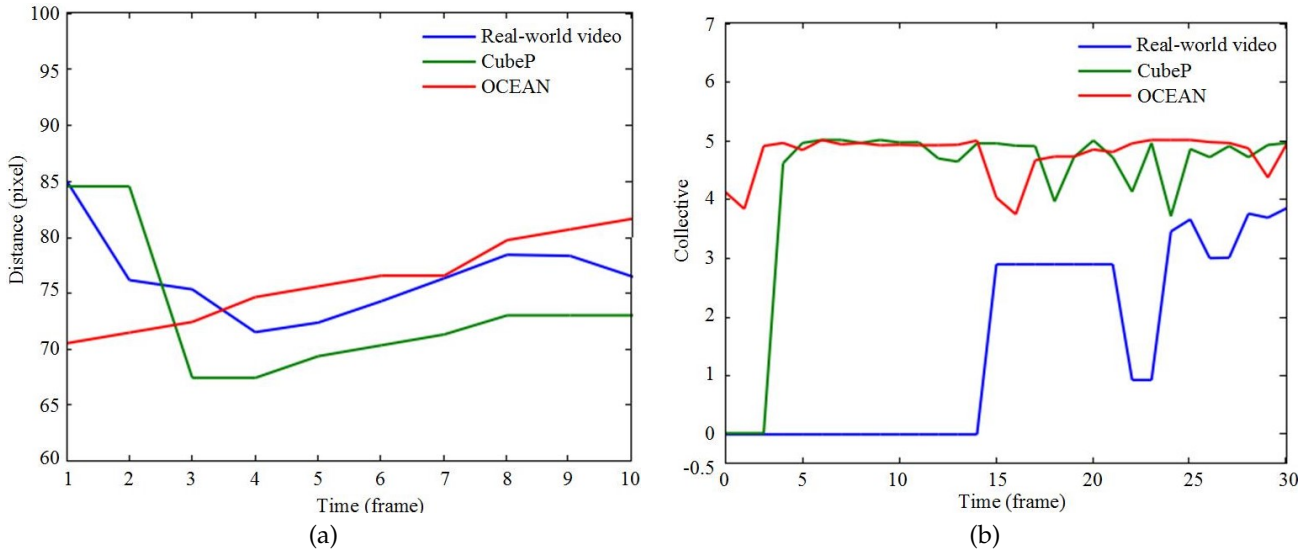


Fig. 12: Comparison of distance and collective between real scenes and simulation results by different models: (a) Distance between individual No. 1 and individual No. 2 in the grass scenario of Figure 11. (b) Collectiveness in the room scenario of Figure 11.

individual moves slower than before, and physical strength consumption per unit time of this individual is reduced. When his heart rate drops, according to James-Lange theory, the emotional experience is reduced. Therefore, the emotion of individual with 100000J initial value of physical strength consumption is less than the emotion of the individual with 0J initial value of physical strength consumption.

As shown in Figure 8, physical strength consumptions of all three individuals change over time. Before the hazard occurs, all the individuals move at the same speed, and the speed of their physical strength consumption is the same. However, when individuals become panicked, the speed of physical strength consumption increases significantly. The more panicked the individual is, the more physical strength he consumes.

The moving speed of all three individuals with the same initial values of physical strength consumption is presented in Figure 9. The moving speed with different initial values of physical strength consumption are presented in Figure 10. Both emotion and physical strength affect the moving speed of individuals. The more panicked an individual is, the faster is his moving speed. The less physical strength consumption of an individual is, the faster is his moving speed. Emotion affects individuals' moving direction by driving them to run away from the hazard. When individuals are far from the hazard and arrive in a safe place, they are not panicked and their moving speed is restored to normal level.

4.2 Comparisons

To validate our approach, we compare the simulation results obtained by different methods with real-world crowd evacuation videos. The trend of simulation results obtained by our CubeP model are more similar to that of the real-world videos.

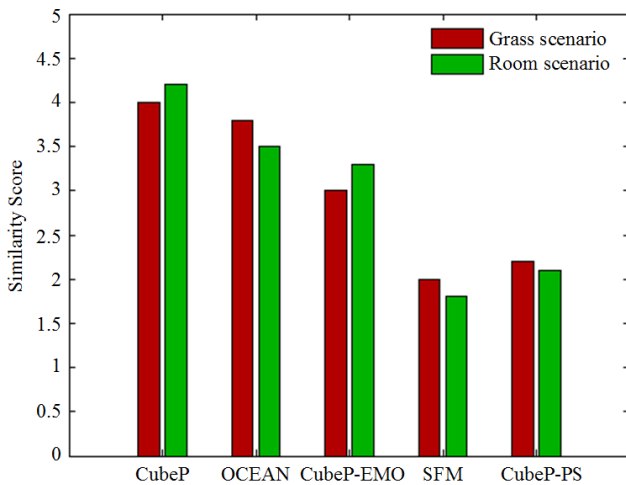


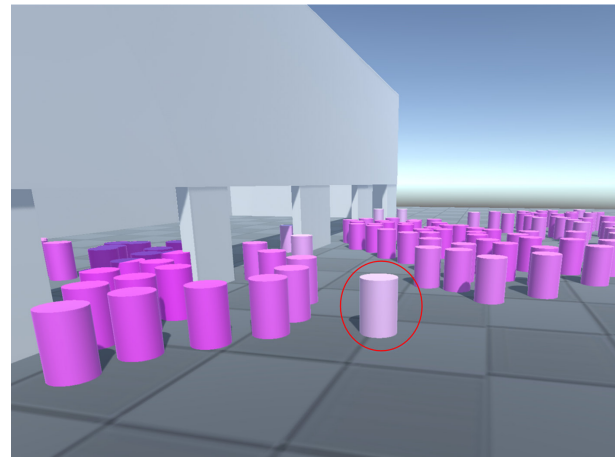
Fig. 13: Comparison of similarity scores for movement state (higher values indicate greater similarity). We compare the movement state in the original videos with that in crowd simulation results by different algorithms.

The comparison between real scenes and the corresponding simulation results are presented in Figure 11. We take

two different real-world scenarios (chosen from the public UMN dataset [58]) as examples and detailed results can be seen in the supplementary video. The CubeP model is compared with the SIR model based on the OCEAN model, which is denoted as the OCEAN model for convenience [7]. We determine the trajectories of all the individuals in the real-world video and assign the initial movement state to the CubeP and OCEAN models. Therefore, we can predict the trajectories of these individuals and compare them with the actual ones.



(a) Real-world video



(b) Simulation by the CubeP model

Fig. 14: Crowd simulation in the case of mobile phone explosion on the subway in the Shanghai Metro Line 8 by the CubeP model

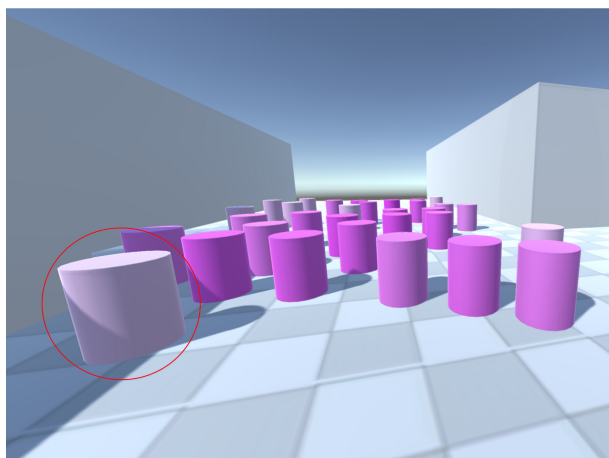
In the grass scenario, individual No. 1 moves faster than individual No. 2, and individual No. 1 moves closer to individual No. 2 (Figure 11a). The simulation result obtained by the CubeP model in the grass scenario is more realistic than that obtained by the OCEAN model. The reason is that the speed is influenced by physical strength in the CubeP model. If an individual has consumed more physical strength than other individuals, his moving speed decreases, and other individuals move faster than he does. Thus, simulating the situation is easy when one individual gets closer to another.

In the room scenario, some individuals are marked with

red circles in the simulation results obtained by the OCEAN model (Figure 11f). The moving direction and moving speed of these individuals are almost the same. The collectiveness of the trajectories by the OCEAN model is much higher than that of the real scene. The simulation result by the CubeP model conforms to the real-world video. The reason is that the emotion mechanism of the CubeP model changes the moving direction of individuals and drives them to move away from the hazard. Meanwhile, the physical strength influences the individual's speed.



(a) Real-world video



(b) Simulation by the CubeP model

Fig. 15: Crowd simulation of shooting at the British Parliament building on March 22, 2017 by the CubeP model

We use entropy metric to evaluate the trajectories of different simulation algorithms on different scenarios (see Table 3) [59]. The social force model is denoted as SFM. The CubeP model only considering the emotion factor is denoted as CubeP-EMO. The CubeP model only considering the physical strength factor is denoted as CubeP-PS. This table shows that simulation results by the CubeP model are more similar to real-world videos than other models.

For each scenario, a user study is performed and participants are asked to compare the movement state in the original videos with the movement state in crowd simulation results (Figure 13). Table 3 and Figure 13 show that the simulated moving trends of the CubeP model are more

similar to that of real-world videos than other models. At the same time, the results also show that both physical strength and emotion play key roles in improving the simulation results. A rational approach is to combine physical strength and emotion to determine the movement of each individual.

TABLE 3: Entropy metric for different simulation algorithms on different scenarios. A lower value of entropy metric implies improved similarity with respect to the real-world crowd videos [60].

Scenario	CubeP	OCEAN	CubeP-EMO	CubeP-PS	SFM
Grass	3.3868	3.4290	3.43330	4.0256	4.2955
Room	5.3939	5.4632	5.5033	6.0796	6.1767

We take two real scenarios as examples to verify our proposed crowd simulation method. Crowd simulation by the CubeP model after mobile phone explosion on the subway in the Shanghai Metro Line 8 is presented in Figure 14. Crowd simulation of shooting in the British Parliament building on March 22, 2017 by the CubeP model is presented in Figure 15. We show the spread of the panic emotion in both scenarios. The color of the cylinders represent the emotional intensity of the individuals. From our simulation results and Figure 16, we can see that both the overall moving trend and the process of emotional contagion are similar to that in the recorded real-world crowd videos.

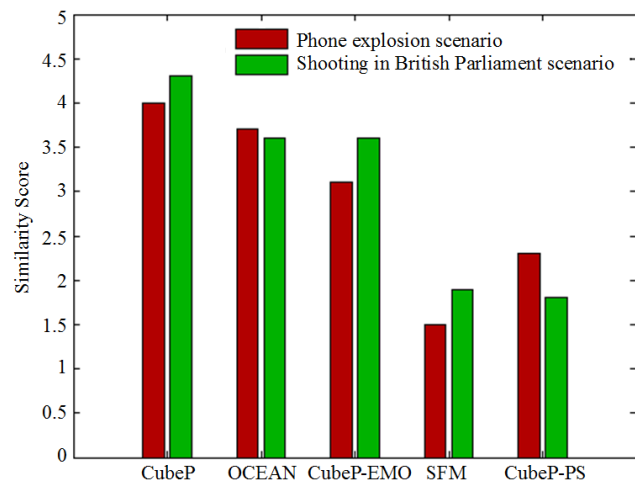


Fig. 16: Comparison of similarity scores for movement state and the process of emotional contagion (higher values indicate greater similarity). A user study is performed and participants are asked to compare the movement state and process of emotional contagion in the original videos with that in crowd simulation results by different algorithms.

4.3 Application of the CubeP model in various virtual scenarios

The CubeP model can be applied in different virtual scenarios. Subway station and crossroad are crowded and the probability of hazard occurrence in these scenarios is very high. We simulate hazard occurring in these scenarios and

three examples are shown. Figure 17 shows crowd simulation at the higher level of the subway station. Figure 18 shows crowd simulation at the lower level of the subway station. Figure 19 shows crowd simulation at a crossroad. We show the process containing hazard occurring, individuals running away from the hazard, emotional contagion, and the attenuation of moving speed. More detail can be seen in the supplementary video. Our simulation results can provide the evidence for the government decision to deal with emergency situations.



Fig. 17: Crowd simulation at the higher level of a subway station. After the hazard occurs, the emotional contagion in our model begins to work at the same time. Although the direct impact of the hazard is limited, the hazardous area grows through emotional contagion among individuals and the number of individuals who run away from the hazard increases.



Fig. 18: Crowd simulation at the lower level of a subway station at the 104th frame. Before the hazard occurs, passengers arrive and leave the station normally. After the hazard occurs, some individuals run away from it and some individuals go upstairs to the top of the subway station.



Fig. 19: Crowd simulation at a crossroad. At the lower left corner, a car explodes and the red area represents the range of influence of the hazard. Individuals on the left run away from the hazard. Individuals on the right are not affected by the hazard.

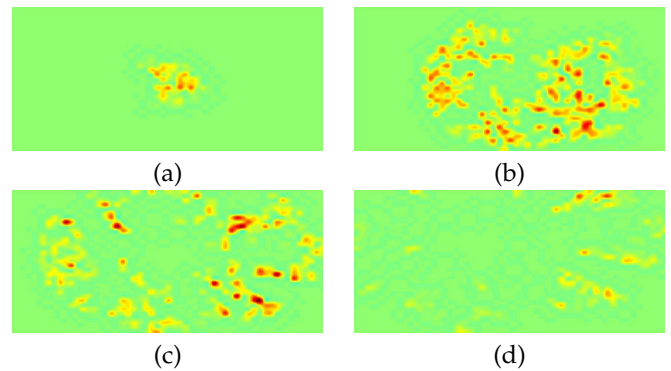


Fig. 20: Panic emotion heat maps of the virtual scene: (a) heat map at the 13th frame, (b) heat map at the 29th frame, (c) heat map at the 57th frame, (d) heat map at the 120th frame. The red area is more panicked than the green area in the heat map. The deeper the color is, the more panicked the area is.

Panic emotion heat maps of the crowd in a virtual scene are presented in Figure 20. Although the direct impact of the hazard is limited, the panic area grows through the emotional contagion mechanism in the CubeP model. When individuals are far from the hazard, panic emotion attenuates. As accidents may happen in public places randomly, we can take preventive action in advance and reduce loss by predicting the panic area accurately.

The panic emotion heat maps of crowd simulations at the crossroad scenario by the CubeP and OCEAN models are presented in Figure 21. The individuals in the CubeP model simulation results are more panicked than those in the OCEAN model simulation results. The intensity of panic emotion calculated by the OCEAN model is lower than that by the CubeP model. The reason is that the CubeP model considers not only emotional contagion among individuals, but also the impact of physical strength on emotion. The CubeP model represents a comprehensive description of

individual emotion and is more conducive to the spread of panic emotion than the OCEAN model. Therefore, the simulation results by the CubeP model is more reasonable for emergency situations.

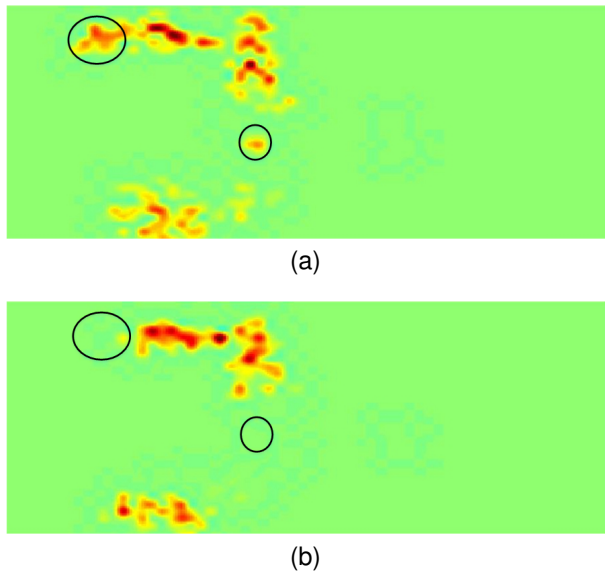


Fig. 21: The panic emotion heat maps of crowd simulations at 185th frame of the crossroad scenario: (a) heat map of the CubeP model crowd simulation result, and (b) heat map of the OCEAN model crowd simulation result. The red area is more panicked than the green area in the heat map. The deeper the color is, the more panicked the area is. We highlight the same area of the two simulation results. The individuals in the CubeP model simulation result are more panicked than the individuals in the OCEAN model simulation results.

5 CONCLUSION AND LIMITATIONS

In contrast to traditional individual behavior models that consider only physiological, psychological, or physical aspects, in this paper, we propose a comprehensive model for emergency crowd simulation by combing all these three aspects together. We not only present physical strength and emotion calculation, but also delineate the relationship between them. We make a comprehensive analysis of physical strength and emotion. Finally, physical strength and emotion determine the movement of each individual. In addition, individual movements affect individual physical strength and emotion emphasizing the interaction of individual physiological, psychological, and physical factors. Our proposed model is verified by simulations, and it is compared with real-world videos and previous approaches. Results have shown that our proposed model can reliably generate realistic group behavior. It can also predict the changes of physical strength and emotion of a crowd in an emergency situation.

However, our model has several limitations. Although the CubeP model can generate realistic crowd movement, the emotion and physical strength of the crowd in an emergency scene cannot be obtained directly. Our model can only infer them during the simulation. Thus, the initial state of our model is difficult to determine and it is usually

time consuming. In the future, we plan to use the latest wearable equipment to collect these data and provide a new method that can quickly and accurately determine the initial state. Furthermore, at present, our model mainly focuses on emergency scenarios. In future work, we aim to extend the CubeP model to common situations.

REFERENCES

- [1] X. Wang, "Understanding collective crowd behaviors: Learning a mixture model of dynamic pedestrian-agents," in *Computer Vision and Pattern Recognition*, 2012, pp. 2871–2878.
- [2] M. Xu, H. Jiang, X. Jin, and Z. Deng, "Crowd simulation and its applications: Recent advances," *Journal of Computer Science and Technology*, vol. 29, no. 5, pp. 799–811, 2014.
- [3] M. Xu, Y. Wu, P. Lv, H. Jiang, M. Luo, and Y. Ye, "misfm: On combination of mutual information and social force model towards simulating crowd evacuation," *Neurocomputing*, vol. 168, pp. 529–537, 2015.
- [4] M. Zhang, M. Xu, L. Han, Y. Liu, P. Lv, and G. He, "Virtual network marathon with immersion, scientificness, competitiveness, adaptability and learning," *Computers & Graphics*, vol. 36, no. 3, pp. 185–192, 2012.
- [5] J. Koo, B.-I. Kim, and Y. S. Kim, "Estimating the effects of mental disorientation and physical fatigue in a semi-panic evacuation," *Expert Systems with Applications*, vol. 41, no. 5, pp. 2379–2390, 2014.
- [6] D. M. Buchner, E. B. Larson, E. H. Wagner, T. D. Koepsell, and B. J. De Lateur, "Evidence for a non-linear relationship between leg strength and gait speed," *Age and ageing*, vol. 25, no. 5, pp. 386–391, 1996.
- [7] F. Durupinar, U. Gdkbay, A. Aman, and N. I. Badler, "Psychological parameters for crowd simulation: From audiences to mobs," *IEEE transactions on visualization and computer graphics*, vol. 22, no. 9, pp. 2145–2159, 2016.
- [8] D. Helbing, I. Farkas, and T. Vicsek, "Simulating dynamical features of escape panic," *Nature*, vol. 407, no. 6803, pp. 487–490, 2000.
- [9] S. A. Stuelvel, N. Magnenat-Thalmann, D. Thalmann, V. D. S. Af, and A. Egges, "Torso crowds," *IEEE Transactions on Visualization and Computer Graphics*, vol. 23, no. 7, p. 1823, 2017.
- [10] J. W. Kalat, *Biological psychology (10th ed.)*. Cengage Learning, 2007.
- [11] S. Kim, S. J. Guy, D. Manocha, and M. C. Lin, "Interactive simulation of dynamic crowd behaviors using general adaptation syndrome theory," in *ACM SIGGRAPH Symposium on Interactive 3d Graphics and Games*, 2012, pp. 55–62.
- [12] Y. Li, M. Christie, O. Siret, and R. Kulpa, "Cloning crowd motions," in *Proceedings of the 11th ACM SIGGRAPH / Eurographics conference on Computer Animation*, 2012, pp. 201–210.
- [13] M. Kapadia, I. K. Chiang, T. Thomas, and N. I. Badler, "Efficient motion retrieval in large motion databases," in *ACM SIGGRAPH Symposium on Interactive 3d Graphics and Games*, 2013, pp. 19–28.
- [14] F. Durupinar, N. Pelechano, J. Allbeck, U. Gudukbay, and N. I. Badler, "How the ocean personality model affects the perception of crowds," *IEEE Computer Graphics and Applications*, vol. 31, no. 3, pp. 22–31, 2011.
- [15] A. Gmez, L. Lpez-Rodrguez, H. Sheikh, J. Ginges, L. Wilson, H. Waziri, A. Vzquez, R. Davis, and S. Atran, "The devoted actor's will to fight and the spiritual dimension of human conflict," *Nature Human Behaviour*, vol. 1, pp. 673–679, 2017.
- [16] S. J. Guy, J. Chhugani, S. Curtis, P. Dubey, M. Lin, and D. Manocha, "PLEdistrans: a least-effort approach to crowd simulation," in *Proceedings of the 2010 ACM SIGGRAPH/Eurographics symposium on computer animation*. Eurographics Association, 2010, pp. 119–128.
- [17] S. Kim, S. J. Guy, W. Liu, R. W. H. Lau, M. C. Lin, and D. Manocha, "Predicting pedestrian trajectories using velocity-space reasoning," *International Journal of Robotics Research*, vol. 34, no. 2, pp. 201–217, 2015.
- [18] N. Roy, P. Newman, and S. Srinivasa, *Modeling and Prediction of Pedestrian Behavior Based on the Sub-Goal Concept*. MIT Press, 2014.
- [19] S. Kim, A. Bera, A. Best, R. Chabra, and D. Manocha, "Interactive and adaptive data-driven crowd simulation," in *2016 IEEE Virtual Reality (VR)*, March 2016, pp. 29–38.
- [20] H. L. Kang, M. G. Choi, Q. Hong, and J. Lee, "Group behavior from video: a data-driven approach to crowd simulation," in *ACM Siggraph/eurographics Symposium on Computer Animation, SCA 2007, San Diego, California, Usa, August, 2007*, pp. 109–118.

- [21] I. Karamouzas, N. Sohre, R. Narain, and S. J. Guy, "Implicit crowds: optimization integrator for robust crowd simulation," *Acm Transactions on Graphics*, vol. 36, no. 4, pp. 1–13, 2017.
- [22] S. Yi, H. Li, and X. Wang, "Pedestrian behavior modeling from stationary crowds with applications to intelligent surveillance," *IEEE transactions on image processing*, vol. 25, no. 9, pp. 4354–4368, 2016.
- [23] J. Kim, Y. Seol, T. Kwon, and J. Lee, "Interactive manipulation of large-scale crowd animation," *ACM Transactions on Graphics (TOG)*, vol. 33, no. 4, p. 83, 2014.
- [24] T. Feng, L. F. Yu, S. K. Yeung, K. K. Yin, and K. Zhou, "Crowd-driven mid-scale layout design," *Acm Transactions on Graphics*, vol. 35, no. 4, p. 132, 2016.
- [25] N. M. Joseph, and N. M. Joseph, "Zootopia crowd pipeline," in *ACM SIGGRAPH*, 2016, p. 59.
- [26] M. Zucker, J. Kuffner, and M. Branicky, "Multipartite RRTs for rapid replanning in dynamic environments," in *Robotics and Automation, 2007 IEEE International Conference on*. IEEE, 2007, pp. 1603–1609.
- [27] B. Kluge and E. Prassler, "Reflective navigation: Individual behaviors and group behaviors," in *Robotics and Automation, 2004. Proceedings. ICRA'04. 2004 IEEE International Conference on*, vol. 4. IEEE, 2004, pp. 4172–4177.
- [28] H. Wang, J. Ondřej, and C. OSullivan, "Trending paths: A new semantic-level metric for comparing simulated and real crowd data," *IEEE transactions on visualization and computer graphics*, vol. 23, no. 5, pp. 1454–1464, 2017.
- [29] A. Bera, S. Kim, T. Randhavane, S. Pratapa, and D. Manocha, "GImp- realtime pedestrian path prediction using global and local movement patterns," in *IEEE International Conference on Robotics and Automation*, 2016, pp. 5528–5535.
- [30] X. Wang, N. Liu, S. Liu, Z. Wu, M. Zhou, J. He, P. Cheng, C. Miao, and N. M. Thalmann, "Crowd formation via hierarchical planning," in *ACM SIGGRAPH Conference on Virtual-Reality Continuum and ITS Applications in Industry*, 2016, pp. 251–260.
- [31] T. Weiss, A. Litteneker, C. Jiang, and D. Terzopoulos, "Position-based multi-agent dynamics for real-time crowd simulation," in *Proceedings of the ACM SIGGRAPH/Eurographics Symposium on Computer Animation*. ACM, 2017, p. 27.
- [32] L. He, J. Pan, S. Narang, and D. Manocha, "Dynamic group behaviors for interactive crowd simulation," in *ACM Siggraph/eurographics Symposium on Computer Animation*, 2016, pp. 139–147.
- [33] M. Xu, Y. Wu, Y. Ye, I. Farkas, H. Jiang, and Z. Deng, "Collective crowd formation transform with mutual informationbased runtime feedback," *Computer Graphics Forum*, vol. 34, no. 1, pp. 60–73, 2015.
- [34] F. Belkhouche, "Reactive path planning in a dynamic environment," *IEEE Transactions on Robotics*, vol. 25, no. 4, pp. 902–911, 2009.
- [35] S. Patil, J. Van Den Berg, S. Curtis, M. C. Lin, and D. Manocha, "Directing crowd simulations using navigation fields," *IEEE transactions on visualization and computer graphics*, vol. 17, no. 2, pp. 244–254, 2011.
- [36] R. Kulpa, A.-H. Olivier, J. Ondřej, and J. Pettré, "Imperceptible relaxation of collision avoidance constraints in virtual crowds," *ACM Transactions on Graphics (TOG)*, vol. 30, no. 6, p. 138, 2011.
- [37] R. Gayle, A. Sud, E. Andersen, S. J. Guy, M. C. Lin, and D. Manocha, "Interactive navigation of heterogeneous agents using adaptive roadmaps," *IEEE Transactions on Visualization and Computer Graphics*, vol. 15, no. 1, pp. 34–48, 2009.
- [38] A. Sud, E. Andersen, S. Curtis, M. C. Lin, and D. Manocha, "Real-time path planning in dynamic virtual environments using multiagent navigation graphs," *IEEE transactions on visualization and computer graphics*, vol. 14, no. 3, pp. 526–538, 2008.
- [39] A. Golas, R. Narain, S. Curtis, and M. C. Lin, "Hybrid long-range collision avoidance for crowd simulation," *IEEE transactions on visualization and computer graphics*, vol. 20, no. 7, pp. 1022–1034, 2014.
- [40] T. Bosse, M. Hoogendoorn, M. C. Klein, J. Treur, C. N. Van Der Wal, and A. Van Wissen, "Modelling collective decision making in groups and crowds: Integrating social contagion and interacting emotions, beliefs and intentions," *Autonomous Agents and Multi-Agent Systems*, pp. 1–33, 2013.
- [41] M. Xu, Z. Pan, M. Zhang, P. Lv, P. Zhu, Y. Ye, and W. Song, "Character behavior planning and visual simulation in virtual 3d space," *IEEE Multimedia*, vol. 20, no. 1, pp. 49–59, 2013.
- [42] W. O. Kermack and A. G. McKendrick, "Contributions to the mathematical theory of epidemics. III. further studies of the problem of endemicity," *Proceedings of the Royal Society of London. Series A, Containing Papers of a Mathematical and Physical Character*, vol. 141, no. 843, pp. 94–122, 1933.
- [43] L. Zhao, H. Cui, X. Qiu, X. Wang, and J. Wang, "SIR rumor spreading model in the new media age," *Physica A: Statistical Mechanics and its Applications*, vol. 392, no. 4, pp. 995–1003, 2013.
- [44] J. Tsai, E. Bowring, S. Marsella, and M. Tambe, "Empirical evaluation of computational fear contagion models in crowd dispersions," *Autonomous agents and multi-agent systems*, vol. 27, no. 2, pp. 200–217, 2013.
- [45] S. H. White, A. M. Del Rey, and G. R. Sánchez, "Modeling epidemics using cellular automata," *Applied Mathematics and Computation*, vol. 186, no. 1, pp. 193–202, 2007.
- [46] J.-h. Wang, S.-m. Lo, J.-h. Sun, Q.-s. Wang, and H.-l. Mu, "Qualitative simulation of the panic spread in large-scale evacuation," *Simulation*, vol. 88, no. 12, pp. 1465–1474, 2012.
- [47] L. Fu, W. Song, W. Lv, and S. Lo, "Simulation of emotional contagion using modified SIR model: a cellular automaton approach," *Physica A: Statistical Mechanics and its Applications*, vol. 405, pp. 380–391, 2014.
- [48] J. Bruneau, A.-H. Olivier, and J. Pettré, "Going through, going around: A study on individual avoidance of groups," *IEEE transactions on visualization and computer graphics*, vol. 21, no. 4, pp. 520–528, 2015.
- [49] W. R. Leonard, "Measuring human energy expenditure: What have we learned from the flex-heart rate method?" *American journal of human biology*, vol. 15, no. 4, pp. 479–489, 2003.
- [50] L. Keytel, J. Goedecke, T. Noakes, H. Hiiloskorpi, R. Laukkanen, L. van der Merwe, and E. Lambert, "Prediction of energy expenditure from heart rate monitoring during submaximal exercise," *Journal of sports sciences*, vol. 23, no. 3, pp. 289–297, 2005.
- [51] S. J. Guy, J. Chhugani, C. Kim, N. Satish, M. Lin, D. Manocha, and P. Dubey, "Clearpath: highly parallel collision avoidance for multi-agent simulation," in *Proceedings of the 2009 ACM SIGGRAPH/Eurographics Symposium on Computer Animation*. ACM, 2009, pp. 177–187.
- [52] J. Nilsson and A. Thorstensson, "Ground reaction forces at different speeds of human walking and running," *Acta Physiologica*, vol. 136, no. 2, pp. 217–227, 1989.
- [53] R. Cross, "Standing, walking, running, and jumping on a force plate," *American Journal of Physics*, vol. 67, no. 4, pp. 304–309, 1999.
- [54] J. M. Burnfield, Y. J. Tsai, and C. M. Powers, "Comparison of utilized coefficient of friction during different walking tasks in persons with and without a disability," *Gait & Posture*, vol. 22, no. 1, p. 82, 2005.
- [55] H. M. Petry and O. Desiderato, "Changes in heart rate, muscle activity, and anxiety level following shock threat," *Psychophysiology*, vol. 15, no. 5, pp. 398–402, 1978.
- [56] J. Shao, K. Kang, C. L. Chen, and X. Wang, "Deeply learned attributes for crowded scene understanding," in *Computer Vision and Pattern Recognition*, 2015, pp. 4657–4666.
- [57] M. Xu, C. Li, P. Lv, N. Lin, R. Hou, and B. Zhou, "An efficient method of crowd aggregation computation in public areas," *IEEE Transactions on Circuits & Systems for Video Technology*, vol. PP, no. 99, pp. 1–1, 2017.
- [58] R. Mehran, A. Oyama, and M. Shah, "Abnormal crowd behavior detection using social force model," in *Computer Vision and Pattern Recognition, 2009. CVPR 2009. IEEE Conference on*, 2009, pp. 935–942.
- [59] A. Lerner, Y. Chrysanthou, A. Shamir, and D. Cohen-Or, "Data driven evaluation of crowds," in *International Workshop on Motion in Games*, 2009, pp. 75–83.
- [60] S. J. Guy, J. V. D. Berg, W. Liu, R. Lau, M. C. Lin, and D. Manocha, "A statistical similarity measure for aggregate crowd dynamics," *Acm Transactions on Graphics*, vol. 31, no. 6, pp. 1–11, 2012.



Mingliang Xu is a professor in the School of Information Engineering of Zhengzhou University, China, and currently is the director of CIISR (Center for Interdisciplinary Information Science Research). His research interests include computer graphics and computer vision. Xu got his Ph.D. degree in computer science and technology from the State Key Lab of CAD&CG at Zhejiang University.



Bing Zhou is currently a professor at the School of Information Engineering, Zhengzhou University, Henan, China. He received the B.S. and M.S. degrees from Xian Jiao Tong University in 1986 and 1989, respectively, and the Ph.D. degree in Beihang University in 2003, all in computer science. His research interests cover video processing and understanding, surveillance, computer vision, multimedia applications.



Chaochao Li is a Ph.D candidate in the School of Information Engineering of Zhengzhou University, China, and his research interest is computer graphics and computer vision. He got his B.S. degree in computer science and technology from the School of Information Engineering of Zhengzhou University.



Dinesh Manocha is currently the Phi Delta Theta/Mason Distinguished Professor of Computer Science at the University of North Carolina at Chapel Hill. He received his Ph.D. in Computer Science at the University of California at Berkeley 1992. Along with his students, Manocha has also received 15 best paper awards at the leading conferences. He has published more than 480 papers and some of the software systems related to collision detection, GPU-based algorithms and geometric computing developed by his group have been downloaded by more than 200,000 users and are widely used in the industry. He has supervised 33 Ph.D. dissertations and is a fellow of ACM, AAAI, AAAS, and IEEE.



Pei Lv is an associate professor in School of Information Engineering, Zhengzhou University, China. His research interests include video analysis and crowd simulation. He received his Ph.D in 2013 from the State Key Lab of CAD&CG, Zhejiang University, China.

He received Distinguished Alumni Award from Indian Institute of Technology, Delhi. He was co-founder of Impulsonic, which was acquired by Valve.



Wei Chen is a professor at the State Key Lab of CAD&CG, Zhejiang University. His research interests is on visualization and visual analysis, and has published more than 30 IEEE/ACM Transactions and IEEE VIS papers. He actively served as guest or associate editors of IEEE Transactions on Visualization and Computer Graphics, IEEE Transactions on Intelligent Transportation Systems, and Journal of Visualization. For more information, please refer to <http://www.cad.zju.edu.cn/home/chenwei/>.



Zhigang Deng is a Full Professor of Computer Science at University of Houston (UH). He is also the Director of Graduate Studies at UH Computer Science Department and the Founding Director of the UH Computer Graphics and Interactive Media (CGIM) Lab. He earned Ph.D. in Computer Science at the Integrated Media System Center (NSF ERC) and Department of Computer Science at the University of Southern California in 2006. He completed B.S. degree in Mathematics from Xiamen University (China),

and M.S. in Computer Science from Peking University (China). His interests are in the broad areas of computer graphics, computer animation, human computer interaction, virtual human modeling and animation, and visual computing for biomedical/healthcare informatics. He is the recipient of ACM ICMI Ten Year Technical Impact Award, UH Teaching Excellence Award, Google Faculty Research Award, UHCS Faculty Academic Excellence Award, and NSFC Overseas and Hong Kong/Macau Young Scholars Collaborative Research Award. Besides the CASA 2014 conference general co-chair and SCA 2015 conference general co-chair, He currently serves as an Associate Editor of several journals including Computer Graphics Forum, and Computer Animation and Virtual Worlds Journal.